

1.4 GHz CONTINUUM SOURCES IN THE HERCULES CLUSTER

J. M. DICKEY

Astronomy Department, University of Minnesota

AND

E. E. SALPETER

Center for Radiophysics and Space Research, Cornell University

Received 1983 October 21; accepted 1984 March 23

ABSTRACT

We have made a continuum survey near 1.4 GHz with the VLA D configuration of three fields, centered on the Hercules Cluster of galaxies (A2151). We give positions and fluxes for 65 sources. Because of the good sensitivity of the data, we now have more reliable positions than previously. There are 21–25 sources associated with galaxies (mostly bright galaxies), and the separation between the radio and optical positions is $\lesssim 5''$ for most cases.

We examined three small rectangles, one near the classical Hercules Cluster center, one north, and one south, which contain some optically bright galaxies and one strongly radio-emitting galaxy each. Two of the three strongly radio-emitting galaxies are head-tail sources, which indicates an intergalactic medium. We suggest that these three regions are physical “subcores” of A2151 containing intergalactic gas. We find five sources with 1.4 GHz flux > 20 mJy, which are *not* associated with any galaxy, in the small area of the three rectangles. We conjecture that these five galaxyless sources are *not* very distant background objects, but are produced by some plasma effect in the subcore medium of the Hercules Cluster. We cannot exclude the alternative, a chance fluctuation in the number of background sources, and will have to test the conjecture in other galaxy clusters. The radio flux correlates well with the 60 μ m flux from *IRAS* for spiral galaxies, but not for ellipticals.

Subject headings: galaxies: clustering — galaxies: intergalactic medium — radio sources: galaxies

I. INTRODUCTION

Radio continuum emission has been measured for a large number of galaxies (Condon and Dressel 1978*a*, 1978*b*; Kotanyi 1980; Kotanyi and Ekers 1983) in the Virgo Cluster. The Hercules Cluster of galaxies (A2151) is also spiral rich, but about 9 times farther away than the Virgo Cluster, and radio continuum data are available for fewer galaxies (Jaffe and Perola 1975, hereafter JP; Perola and Valentijn 1979). The Hercules Cluster is distinguished by two interesting features: (i) Instead of having a single, central core it has two separate cores (A2151 N and S, see Tarengi *et al.* 1980) or even three separate cores (as we shall claim below); (ii) it contains two head-tail radio galaxies and the related evidence for some intergalactic gas (Valentijn and Perola 1978; Valentijn 1979*a*). Some evidence has been presented for the interaction in Virgo of a radio galaxy with the gas outside M87 (Kotanyi and Ekers 1983); this raises the question whether interaction between radio galaxies and the intergalactic gas in A2151 can be detected by studying displacements between radio and optical images. Another question of general interest is, are there radio continuum sources in a galaxy cluster not associated with individual galaxies? If so, are they restricted to the cluster cores?

We have carried out 1.4 GHz observations of A2151 (including some of the N and S extensions) with the VLA (NRAO¹) in the D configuration. This was mainly for the purpose of H I mapping, but we also have some continuum data with modest resolution (scales of $\sim 30''$) but good sensi-

tivity. We are thus able to look for displacements on scales comparable with, but slightly smaller than, optical galaxy images. We have covered three fields, which include most of the southern and northern cores (or “subclumps”) of A2151. Section II gives the methods used, and § III the results for individual sources.

Because of the good sensitivity of our data, the center positions of many radio images can be determined to a small fraction of the beamwidth. With these accurate positions we find the displacements between radio and optical images of most galaxies (§ IV) to be quite small. This fact gives greater statistical significance to radio sources which are *not* found in association with an optical galaxy (§ V). We conjecture that some of these galaxyless sources are *not* very distant objects, but reside in the “subcores” of the Hercules Cluster (§ VI). A comparison with 60 μ m *IRAS* data is given in § VI.

II. OBSERVATIONS

The observations were made in 1983 June and July, using the VLA (Thompson *et al.* 1980) in the D configuration with 24 antennas. The spectral-line observing mode was used, nominally with 32 frequency channels and total bandwidth 25 MHz; in practice we used only 28 channels (separation 0.78 MHz) with a center frequency of 1372.96 MHz. The inner 24 channels were integrated to form a continuum channel, which is discussed here. The spectral-line data will be reported in a following paper, but preliminary analysis shows that no galaxies have strong enough 21 cm line emission to show up on the continuum maps. Three fields were observed; the field centers were

¹ The National Radio Astronomy Observatory is operated by Associated Universities, Inc., under contract with the National Science Foundation.

(1950 coordinates):

R.A. = $16^{\text{h}}02^{\text{m}}40^{\text{s}}$, decl. = $17^{\circ}36'30''$ (10 hr observing),

R.A. = $16^{\text{h}}02^{\text{m}}40^{\text{s}}$, decl. = $17^{\circ}51'00''$ (12 hr observing),

R.A. = $16^{\text{h}}03^{\text{m}}45^{\text{s}}$, decl. = $18^{\circ}16'30''$ (12 hr observing).

The entire primary beam was mapped, but correction for the attenuation of the single-dish pattern severely increased the noise level beyond about $25'$ from the field center (the primary beam shape is approximately Gaussian with FWHP of $32.6'$ at our frequency). The synthesized beam (CLEAN beam) was $46'' \times 43''$. The maps were CLEANed, self-calibrated, and CLEANed again using the standard AIPS programs. Maps were made with pixel size $10''$, and we finally used only the inner 256×256 pixels (field area $42.7' \times 42.7'$). The three mapped squares (side $42.7'$ each) are indicated in Figure 1. Because of the overlap between squares (especially fields 1 and 2), the total area mapped is only $\sim 3,500$ arcmin². Fluxes were calibrated by observing 3C 48 and 3C 286; the bandwidth shape was calibrated by observations of 1607+268, which doubled as the phase calibrator.

The dynamic range obtained was 1000:1 on the first field and close to 2000:1 on the second and third fields, corresponding to rms noise of about 0.6 mJy and 0.3 mJy, respectively. The poorer dynamic range for the observations of the first field was due in part to the slightly shorter observing period, to the use of 23 antennas instead of 24, and in part due to the indirect effects of a strong interference spike at an apparent frequency

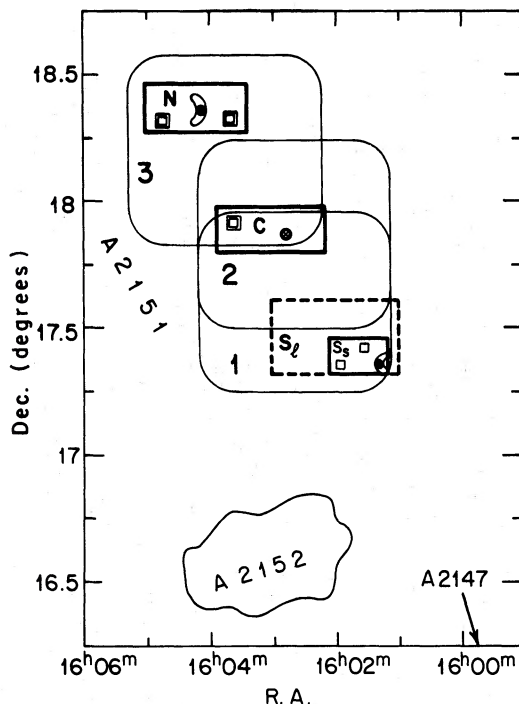


FIG. 1.—An outline of the Hercules Cluster, A2151. The three squares with rounded corners denote the mapped VLA fields 1, 2, and 3. The heavy rectangles marked C and N give the location of two chosen subcores, mapped further in Figs. 3a and 4a. The dashed and solid heavy rectangles marked S_1 and S_2 are two choices for a southern subcore, mapped further in Fig. 5a. Three strong continuum sources associated with bright galaxies are indicated by crosshatched circles, and five strong galaxyless sources by squares (double squares for $S > 50$ mJy). The approximate locations of two other clusters in the Hercules Supercluster are also indicated.

1361.2 MHz. The stability was slightly worse during about 4 hr per field before sunset, but very few data have to be discarded. We estimate that absolute flux values (and relative fluxes of sources measured in different fields) are uncertain by about 10% (at least for weak or extended sources).

III. INDIVIDUAL SOURCES

For each of the three fields (with centers given in § II) we searched for continuum sources in a square of length $42'$. We list in Table 1 all sources with integrated flux S larger than 3 mJy. In each case the coordinates of the source center (cols. [3] and [4]), the integrated flux S (col. [5]), and the approximate size of the source (col. [7]) were obtained from the AIPS Gaussian fitting program. Because of the poor primary beam sensitivity near the corners of each field, and because of noise near very strong sources, we estimate that we miss about 10% of sources with $S > 9$ mJy and about 25% of sources with S between 3 mJy and 9 mJy. Because of their special interest we also list a few sources with $S < 3$ mJy (but do not include them in statistical studies below) if they lie within $40''$ of an optical galaxy on the OW-list discussed in § IV. We also list the “gain factor” (G.F., col. [6]) by which the program multiplies the received flux to correct for the gain pattern of the primary beam (if two fields were used, the smaller value of G.F. is given in col. [6], and the other values in Table 1 are means weighted in favor of the field with the smaller G.F.).

Table 1 contains 65 distinct sources; very few of these (if any) are likely to be spurious noise spikes. The two head-tail sources, #1 and #59—and the entry #66? (a “clump” in the tail of source #59)—are discussed further in § V. In column (2) of Table 1, field 1 refers to the southern field position given in § II, 2 is the central field containing the “classical Hercules Cluster” core, and 3 is the northern field. When three numbers appear in column (7), they are major and minor axis diameters in arcsec (full width at half-power) and the position angle of the major axis (in degrees), after deconvolving the synthesized beam from the Gaussian shape fitted by the AIPS program. For a “nominal point source” (denoted by the absence of numbers in col. [7]) the major and minor axis diameters before deconvolving (obtained from the AIPS Gaussian fit program) usually are between $35''$ and $50''$.

Our fields 1 and 2 overlap sufficiently that a number of sources were observed on two fields. Westerbork data at 21 cm for 18 sources in our Table 1 were already published by JP. These sources are indicated in our Table 1 by a number in parentheses in column (1), which indicates the last digit (following W) in the JP source name (the digits before W can be inferred from the coordinates in our Table 1). Comparison of our data from two fields shows that the positions in our Table 1 are gratifyingly good (unless the source is very extended or complex), with typical errors appreciably less than $5''$ (which is only one-tenth the beamwidth). Comparison with the JP data for the 18 sources in common also shows the absence of any appreciable systematic position offsets: The mean difference between JP and our Table 1 is only $1''.5$ in R.A. and $0''.9$ in decl. The position difference exceeds $6''$ for only three of the 18 sources: for source #12 ($1602+17W2$) the JP position is presumably unreliable because of blending with our source #11, for source #27 ($1603+17W2$) the JP position is presumably poor because the flux is below their completeness limit, and for source #38 ($1604+17W1$) our position is presumably poor because it is near the corner of a field (G.F. = 5.6). Only two additional sources in our Table 1 (#15 and #26; see notes to

TABLE 1
ALL DETECTED SOURCES

| Source No. (1) | Field (2) | R.A. 16 ^h + (3) | Decl. 17 ^o + (4) | Flux S (mJy) (5) | G.F. (6) | Size or Comments ("', "'; °) (7) |
|-----------------------|-----------|----------------------------|-----------------------------|------------------|----------|----------------------------------|
| 1 ^a (1) | 1 | 01 ^m 16.4 | 20 ¹² " | 357 | 7.7 | Head-tail |
| 2 | 2 | 01 18.4 | 55 17 | 4.7 | 3.1 | |
| 3 | 1 | 01 36.1 | 27 35 | 24 | 2.3 | |
| 4 | 1 | 01 44.3 | 23 49 | 8.0 | 2.5 | |
| 5 | 1 | 01 53.8 | 20 23 | 2.9 | 2.9 | |
| 6 | 1 | 02 04.7 | 34 21 | 1.6 | 1.2 | |
| 7 | 1 | 02 07.1 | 20 01 | 22 | 2.5 | |
| 8 ^a (1) | 1, 2 | 02 11.5 | 52 42 | 101 | 1.1 | |
| 9 | 1 | 02 14.3 | 36 24 | 1.3 | 1.1 | |
| 10 | 1, 2 | 02 16.5 | 42 51 | 5.1 | 1.3 | 44, 24; 26 |
| 11 | 1, 2 | 02 20.7 | 50 34 | 7.4 | 1.1 | |
| 12 (2) | 1, 2 | 02 20.8 | 51 20 | 6.0 | 1.1 | |
| 13 (3) | 1, 2 | 02 21.4 | 41 33 | 19 | 1.1 | |
| 14 | 1 | 02 24.7 | 25 55 | 4.9 | 1.4 | |
| 15 (a) ^b | 1 | 02 29.7 | 35 03 | 2.0 | 1.0 | |
| 16 | 1 | 02 32.3 | 28 53 | 1.5 | 1.2 | |
| 17 ^c | 1, 2 | 02 53.2 | 53 25 | ~30? | 1.0 | Complex |
| 18 ^d (4) | 1, 2 | 02 54.1 | 51 54 | 780 | 1.0 | 38, 15; 177 |
| 19 | 1 | 02 57.0 | 33 33 | 2.7 | 1.0 | |
| 20 | 1 | 02 59.1 | 24 57 | 2.3 | 1.5 | |
| 21 | 1, 2 | 03 01.5 | 55 43 | 5.3 | 1.1 | |
| 22 | 1 | 03 02.7 | 16 25 | 10.8 | 3.2 | |
| 23 (1) | 1, 2 | 03 03.9 | 39 51 | 33 | 1.1 | |
| 24 | 2 | 03 08.2 | 53 29 | 3.4 | 1.1 | |
| 25 | 2, 3 | 03 12.9 | 57 56 | 2.0 | 3.2 | |
| 26 (b) ^e | 1, 2 | 03 18.5 | 43 46 | 4.0 | 1.4 | Complex? |
| 27 ^f (2) | 2, 3 | 03 21.8 | 56 12 | ≥ 5.1 | 1.4 | Double? |
| 28 | 1, 2 | 03 29.7 | 50 48 | 9.4 | 1.4 | 20, 7; 33 |
| 29 | 1 | 03 32.9 | 26 30 | 2.6 | 2.0 | |
| 30 | 1 | 03 39.5 | 40 39 | 3.0 | 1.8 | |
| 31 (4) | 1, 2 | 03 41.6 | 48 04 | 12.0 | 1.8 | |
| 32 | 1 | 03 43.8 | 17 56 | 4.1 | 1.8 | |
| 33 | 1, 2 | 03 44.6 | 54 04 | 11.5 | 2.0 | |
| 34 | 1, 2 | 03 45.8 | 51 46 | 3.9 | 1.9 | |
| 35 ^{g,h} (5) | 1, 2 | 03 46.2 | 55 52 | 120 | 2.1 | 14, 12; 155 |
| 36 | 1, 2 | 03 50.3 | 34 57 | 3.9 | 2.1 | |
| 37 | 1 | 03 56.9 | 26 14 | 2.0 | 3.5 | |
| 38 ⁱ (1) | 1 | 04 17.8 | 41 27 | 10.6 | 5.6 | |
| 39 ^j | 1 | 04 18.8 | 37 23 | 9.6 | 5.4 | |
| 40 | 3 | 04 27.6 | 59 22 | 3.7 | 3.0 | |
| 41 ^k | 3 | 04 50.1 | 58 49 | 3.0 | 5.3 | |
| 42 ^l | 2 | 01 21.9 | 10 19 | 7.0 | 10 | |
| 43 (1) | 2 | 01 33.9 | 00 46 | 16 | 2.6 | |
| 44 (1) | 2 | 02 11.0 | 11 25 | 29 | 4.1 | |
| 45 (2) | 2 | 02 21.6 | 06 34 | 32 | 2.1 | |
| 46 | 2 | 02 35.6 | 05 54 | 4.3 | 1.9 | |
| 47 | 3 | 02 44.2 | 19 21 | 1.9 | 1.8 | |
| 48 | 3 | 02 53.2 | 18 15 | 8.5 | 1.5 | 31, 14; 68 |
| 49 | 3 | 02 54.8 | 33 21 | 8.5 | 3.6 | |
| 50 (1) | 2, 3 | 03 11.7 | 03 48 | 9.9 | 1.8 | 21, 6; 117 |
| 51 | 2, 3 | 03 12.1 | 09 15 | 5.9 | 1.3 | |
| 52 | 3 | 03 13.1 | 28 29 | 4.6 | 1.6 | |
| 53 ^{h,j} (2) | 3 | 03 25.4 | 20 08 | 92 | 1.1 | 60, 6; 67 |
| 54 | 3 | 03 37.5 | 21 16 | 1.7 | 1.1 | |
| 55 | 3 | 03 42.5 | 36 32 | 6.1 | 3.1 | |
| 56 | 3 | 03 52.7 | 21 17 | 11.2 | 1.1 | |
| 57 | 3 | 04 00.3 | 18 57 | 5.9 | 1.1 | |
| 58 | 3 | 04 00.8 | 08 22 | 6.1 | 1.2 | |
| 59 ^k (1) | 3 | 04 01.7 | 23 00 | 276 | 1.1 | 20, 8; 145 Wide-angle tail |
| 60 | 3 | 04 13.5 | 23 47 | 9.1 | 1.3 | |
| 61 | 3 | 04 27.2 | 17 40 | 19 | 1.8 | |
| 62 (2) | 3 | 04 31.7 | 08 53 | 40 | 1.6 | 16, 7; 82 |
| 63 ^{h,l} (3) | 3 | 04 42.4 | 19 31 | 326 | 1.7 | 16, 4; 89 |
| 64 | 3 | 04 51.9 | 08 14 | 5.0 | 2.4 | |
| 65 | 3 | 04 57.3 | 22 47 | 9.8 | 2.6 | |
| 66 ^m | 3 | 04 13.9 | 19 23 | ~25? | 1.1 | In "tail" |

Tables 1 and 2) were observed previously at Westerbork at 610 MHz (Perola and Valentijn 1979).

Our flux data from individual fields may suffer from some small calibration errors, since the mean flux for duplicated sources is 4% larger in field 2 than in field 1. However, for all the 18 sources in common between our Table 1 and JP, our mean integrated total flux is only 1% larger than that of JP. There are some individual discrepancies in total flux exceeding 20%, but these are mostly "special cases": For source # 12 the JP flux is 1.3 times our flux, but their value probably includes part of our source # 11; our flux is unreliable for source # 38, which lies near the corner of a field (the JP flux is 19 mJy); for source # 53 the JP flux is only 0.69 times our flux (for the whole extended or double source), but their value probably excludes part of the extension. Flux errors due to "bandwidth smearing" should be appreciable in our data only for sources near the corner of a field. Except for sources which are particularly weak or complex or near a field edge, the integrated fluxes in Table 1 should have errors below 10%. For weak and slightly extended sources, the AIPS fitting program does not give a deconvolved size (a blank in col. [7] in Table 1); even for the stronger sources the stated sizes are not much better than an order-of-magnitude estimate, since the real shape is usually more complex than the assumed Gaussian.

IV. SOURCES ASSOCIATED WITH GALAXIES

Accurate optical magnitudes are available for only relatively few Hercules Cluster galaxies (Bothun 1981), but accurate positions are available for a large number. We shall refer to three different galaxy lists for the area of 3.5×10^3 arcmin² included in our combined three fields (see § II). There are 38 galaxies, all from field Z108 of Zwicky, for which optical redshifts were determined by Tarenghi *et al.* (1979); these will be denoted by T followed by the Z108 galaxy number. A list of 120 galaxies (including the T-list) with morphological types is taken from Dressler (1980) and labeled D. Finally, a list of 269 galaxies (including the D-list), with coordinates accurate to better than 3", was kindly provided to us prior to publication by Okamura and Wakamatsu (1983) (OW-list).

^a This head-tail source in the corner of field 1 is mapped in Fig. 4b; better Westerbork data are given by Valentijn and Perola 1978.

^b Although this source is weak, it is in the center of field 1, and we expect the flux and position to be fairly reliable. Comparison with the Westerbork 610 MHz data gives a spectral index of about +1.0.

^c This source is slightly extended in a complex way and is close to a stronger source (# 18, Fig. 2c); the flux for # 17 is therefore very uncertain.

^d This slightly extended source, the strongest in the Hercules Cluster, is mapped in Fig. 2c.

^e This source is only slightly extended, but in a complex way. Comparison with the Westerbork 610 MHz data gives a spectral index of about +0.1.

^f The quoted flux of 5.1 mJy underestimates the contribution of a second, weaker component.

^g This strong source is slightly extended; it is mapped in Fig. 2b and discussed in §§ V and VI.

^h For # 35, # 53, and # 63, JP had already searched for optical candidates to a fainter limit than the OW-list, but not found any convincing association.

ⁱ Noisy data because sources are near corner of a field.

^j This strong, extended (or possibly double) source is mapped in Fig. 3d and discussed in §§ V and VI.

^k Westerbork data for this wide-angle-tailed source are discussed by Valentijn 1979a; our data are mapped in Fig. 3c.

^l This strong, extended source is mapped in Fig. 3b and discussed in §§ V and VI.

^m This entry in Table 1 (mapped in Fig. 3c) is presumably not an independent object but a condensation in the tail of # 59.

In Table 2 we list again all 28 continuum sources from Table 1 whose centers lie within $40''$ of the optical position of one of the 269 galaxies on the OW-list. If the galaxy is also on the D-list, the D-number and Dressler's description of morphological type are listed, as is Dressler's "approximate magnitude indicator" m . If the galaxy is also on the T-list, the T-number is also given (and the NGC, IC, or UGC number, if available, is underneath). The final column in Table 2 gives θ , the angular separation (in arcsec) between the centers of the radio continuum source and the optical galaxy.

TABLE 2
SOURCES IDENTIFIED WITH GALAXIES

| SOURCE No. | FLUX (mJy) | OW No. | DRESSLER | | | T No. (NGC, IC, or UGC No.) | θ (") |
|-----------------|------------|--------|----------|------|-----|-----------------------------|--------------|
| | | | No. | Type | m | | |
| 1 | 357 | 22 | D7 | E | 12 | T84 (N6034) | 1.9 |
| 4 | 8 | 52 | ... | ... | ... | ... | 21 |
| 5 | 2.9 | 62 | D5 | Sd | 16 | ... | 17 |
| 6 | 1.6 | 71 | D25 | S | 16 | ... | 2.3 |
| 8 ^a | 101 | 84 | D68 | S0/a | 14 | T96S (N6040 A) | 1.5 |
| 9 | 1.3 | 98 | D31 | Sc | 15 | T98 | 14 |
| 12 ^b | 6.0 | 96 | D64 | S0 | 14 | T101 | 8 |
| 15 ^c | 2.0 | 116 | D30 | Sb | 14 | T108 | 5 |
| 16 | 1.5 | 121 | D20 | Sc | 15 | ... | 6 |
| 17 ^d | 30? | 145 | D82 | Sbc | 13 | T112 (N6045) | 4 |
| 18 | 780 | 147 | D62 | E/S0 | 13 | T111 (N6047) | 1.2 |
| 19 | 2.7 | 156 | D24 | Sbc | 14 | T113 (I1173) | 6 |
| 24 | 3.4 | 180 | D155 | Sbc | 15 | T118E (N6050) | 6 |
| 25 | 2.0 | 185 | D90 | S | 15 | ... | 3 |
| 26 ^e | 4.0 | 196 | D39 | SBa | 15 | T120 (I1181) | 5 |
| 27 ^f | 5.1? | 200 | D78 | S0p | 14 | T126 (I1182) | 3 |
| 28 | 9.4 | 222 | D59 | S0 | 16 | T134 (I1185) | 19 |
| 33 | 12 | 245 | ... | ... | ... | ... | 11 |
| 37 | 2.0 | 269 | D12 | E | 16 | ... | 8 |
| 41 | 3.0 | 319 | D85 | S0 | 15 | ... | 17 |
| 47 | 1.9 | 127 | D129 | S | 16 | ... | 5 |
| 52 | 4.6 | 175 | D142 | Sc | 15 | ... | 2.1 |
| 54 | 1.7 | 233 | D128 | Sb | 13 | T136 (U10195) | 13 |
| 57 | 5.9 | 264 | D126 | Sa | 14 | T144 (I1189) | 3 |
| 59 | 276 | 263 | D134 | E/S0 | 14 | T145 (N6061) | 1.3 |

NOTE.—For sources which have been identified with a galaxy both here and at Westerbork, we give the separation between optical and radio both for our VLA data, θ_A , and for the Westerbork data, θ_W , if either exceeds $10''$.

^a Both here and at Westerbork this source is closely identified with the southern component of NGC 6040, an Sa galaxy, and not with the northern Sc companion.

^b $\theta_A = 8''$, $\theta_W = 12''$. Source # 11 (without an optical galaxy counterpart) is nearby.

^c $\theta_A = 5''$, $\theta_W = 18''$.

^d Although this source is close to the much stronger source # 18 (NGC 6047), its association with NGC 6045 seems fairly secure.

^e $\theta_A = 5''$, $\theta_W = 18''$. This source is slightly extended, but its main component is definitely associated with IC 1181 (variously classified as S0p to SBa) rather than IC 1178 (classified as Ep to S0), which is $29''$ away.

^f $\theta_A = 3''$, $\theta_W = 14''$. This source (slightly extended) is identified with IC 1182, a peculiar S0 galaxy with a blue jet which points roughly in the direction of our source 35 ($\sim 6'$ away).

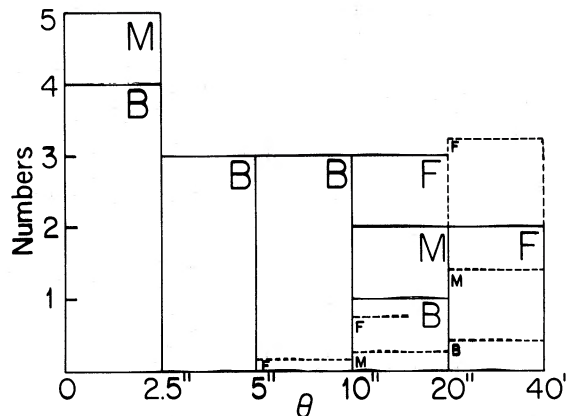


FIG. 2.—Number of observed sources (solid histogram) at various angular distances θ from the optical centers of galaxies in the three fields. B, M, and F denote the three lists of optically "bright," "medium," and "faint" galaxies described in the text. The dashed histogram refers to expected numbers of unrelated background sources.

Sixteen of the 28 sources have integrated flux $S \geq 3$ mJy. For these, Figure 2 gives the histogram of number of sources with θ in various annuli, separately for "bright galaxies" (B, the 38 on the T-list), "medium" (M, the 82 galaxies on the D-list but not on the T-list), and "faint" (F, the 149 galaxies on the OW-list but not on the D-list). Also shown (dashed) are the expected number of physically unrelated background sources which are projected onto the various annuli (see § V). The three sources with θ between $20''$ and $40''$ are likely to be such background sources. The contamination from background sources is fairly small for $10'' < \theta < 20''$ and negligible for $\theta < 10''$. The fact that $\theta \lesssim 5''$ for many sources supports the assertion of § III that source positions are often good to better than about one-tenth of the synthesized beamwidth of $\sim 50''$. For the 12 sources in Table 2 with $1.3 \text{ mJy} < S < 3 \text{ mJy}$ the distribution is shifted to slightly larger values of θ , partly because the position error is greater for these weaker continuum sources and partly because background contamination is more important. As discussed in the notes to Tables 1 and 2, the increased VLA sensitivity has led to an improved positional accuracy for many sources and—most important—the increased accuracy has usually led to a decrease in θ , the measured separation between the radio and optical image centers. It is very likely that $\theta \lesssim 15''$ for most sources which are physically associated with an optical galaxy.

Few of the 21 sources with $\theta < 15''$ in Table 2 are likely to be spurious (i.e., few, if any, are unrelated background sources or merely noise spikes), and we have one of the two ingredients for constructing a joint radio-optical luminosity function for a cluster with reasonably good statistics. Unfortunately, at the moment we do not have accurate optical magnitudes for many of the galaxies, nor even accurate magnitude limits for the D- and OW-lists. The mean magnitude difference between the B- and M-lists, and between the M- and F-lists, is probably ~ 1.5 mag each. Defining a "radio detection" by the requirements $S > 1.3 \text{ mJy}$ and $\theta < 15''$ in Table 2, we have the following, rather spectacular, detection statistics: of the 38 B-galaxies (T-list) we detected 14, of the 82 M-galaxies we detected six, but of the 149 F-galaxies (solely on the OW-list) we detected only a single one (whose Hubble type is not known)! The Hubble types assigned by Dressler (1980) differ slightly from those of Tarenghi *et al.* (1979), but if S0 and S0/a galaxies are included

TABLE 3
DETECTION STATISTICS FOR VARIOUS GALAXY LISTS

| OPTICAL SAMPLE | Types = Total Number = | BRIGHT (T-LIST) | | MEDIUM (D-LIST - T-LIST) | | FAINT (OW-LIST) | |
|--|---------------------------|---------------------|------------------|--------------------------|-------------|-----------------|-------------|
| | | E and S0 18 (15) | Sa-Sd 20 (16) | E and S0 37 (34) | Sa-Sd 45 | E and S0 74 | Sa-Sd 75 |
| 21 cm detections ($S > 1.3$ mJy) | | 3 | 7 | 5 | 8 | 0 or 1 | 1 or 0 |
| Predicted (Aurionemma <i>et al.</i> 1977) | | 3.3 | 3.5 | 1.3 | 1.7 | 0.5 | 0.5 |
| 21 cm detections ($S > 50$ mJy) | | 3 | 1 | 0 | 0 | 0 | 0 |
| Predicted (Aurionemma <i>et al.</i> 1977) | | 0.9 | 0.9 | 0.06 | 0.08 | 0.004 | 0.004 |
| 60 μ m detections | | 1 | 8 | 1 | 11 | ... | ... |
| 60 μ m and 21 cm detections | | 1 | 6 | 0 | 6 | ... | ... |

with ellipticals (E), the galaxy lists contain similar numbers of ellipticals and spirals (Sp). The breakdown of detected galaxies is given in the second row of Table 3. We also have qualitative confirmation of a trend noted before (see, e.g., Jaffe and Perola 1976; Valentijn, Perola, and Jaffe 1977; Valentijn 1980), namely, that the ratio of radio to optical luminosity L_{op} decreases with decreasing L_{op} : We assume that mean optical luminosities decrease by a factor of 16 from B-galaxies to F. The number of detections for $S > 50$ mJy for B and $S > 1.3$ mJy for F are given in the third and second rows of Table 3. A comparison with predictions from the luminosity function of Aurionemma *et al.* (1977) is given in § VI.

From our data and the references mentioned above, we can make two empirical assertions: (1) In Figure 2 for the distribution of radio-optical separations θ , we found many more sources with $\theta < 10''$ than with $10'' < \theta < 20''$ (especially for bright galaxies). Cases with $\theta \geq 40''$ are therefore unlikely to indicate true physical association. (2) A galaxy in the Hercules Cluster area which is too faint optically to be included in the OW-list is very unlikely to emit radio continuum with $S > 3$ mJy (by extrapolation from the F-galaxies which are included in the OW-list).

V. SOURCES WITHOUT GALAXIES AND THE CLUSTER "SUBCORES"

Of the 65 fairly distinct sources in Table 1, 37 with $S \geq 3$ mJy are farther than $40''$ from any galaxy on the OW-list. As asserted in § IV, most of these 37 sources are likely to be unassociated with galaxies in the Hercules Cluster. Many of the sources are presumably background sources (very large radio luminosity and redshift $z \gg z_{\text{Herc}} = 0.036$), but the question is how many (if any) are situated in the Hercules Cluster without association with a regular galaxy? To minimize the importance of background sources we want to restrict ourselves to a smaller area where the surface density of cluster galaxies is high, and we summarize first the detailed geography of this cluster:

From optical data on galaxies we know that the classical Hercules Cluster (A2151) is very "clumpy" and somewhat irregular in shape but is generally elongated in a N-S direction and is part of a supercluster which is even more extended in the N-S direction (see A2152 and A2147 off scale on Fig. 1). The most prominent clump, as outlined by bright galaxies, is shown schematically in Figures 1 and 3a; it coincides approximately with the "classical Hercules Cluster core" and will be referred

to as C. As seen in Tables 1 and 2 and Figure 3a, the strongest radio continuum source of A2151 is also located in this region, source #18 located within $2''$ of the bright elliptical galaxy T111 (NGC 6047). The optical data also show two other, slightly less prominent clumps, or "subcores," which we denote by N and S, respectively, and display schematically in Figures 1, 4a, and 5a. Our choice for the rectangle N is fairly unique, but the choice for the southern subcore depends on just how many bright galaxies one wants to include; our rectangles S_s and S_1 are near the small and the large end of the range of choices. From velocity data Tarenghi *et al.* (1980) have argued that our clumps C and S may be one dynamical unit, and clump N may be the center of another dynamical unit. We defer any discussion of dynamics to a later paper and discuss here only phenomenological "clumping," using the following statistical data: The combined area of our three overlapping square fields (before "rounding the corners" of the squares), which cover most of the cluster A2151, is 3500 arcmin², and 38 bright galaxies (the T-list) are in this area. The sum of the three rectangles in Figures 1, 3a, 4a, and 5a contains 20% of this total area (for the choice S_s), but 23 of the 38 bright galaxies on the T-list; for the choice S_1 the rectangles contain 38% of the area, but 26 of the 38 bright galaxies.

The prominence of the galaxy clumps N and S_s has a counterpart in the radio continuum data, since each contains a very strong head-tail or wide-angle-tailed source (Valentijn 1979b). These are source #59 in N, centered on the elliptical galaxy T145, and source #1 in S, centered on the elliptical T84 (NGC 6034). The geography of S is somewhat complicated because the bright spirals are more spread out than the clump of radio continuum sources: the small S_s contains five radio sources above 2.5 mJy, the large S_1 contains only one additional one (#19).

Contour plot details for some of the sources in our rectangles C, N, and S_s are given in Figures 3, 4, and 5 (the head-tail source in S_s , Fig. 5b, is unfortunately near an outside corner of field 1, and the data are noisy). The three rectangles occupy 6.9%, 7.9%, and 5.3% (or 23.1% for choice S_1), respectively, of the total area 3.5×10^3 arcmin² of the combined fields. The observed distribution of flux S for the 37 sources without galaxies is given in Table 4, separately for C+N+S and for the remaining 80% (or 72%) of the area outside these clumps. The expected number of background sources, completely unassociated with the Hercules Cluster, can be obtained from the source count formulae by Oosterbaan (1978) and by Condon and Mitchell (1982). These expected numbers, after

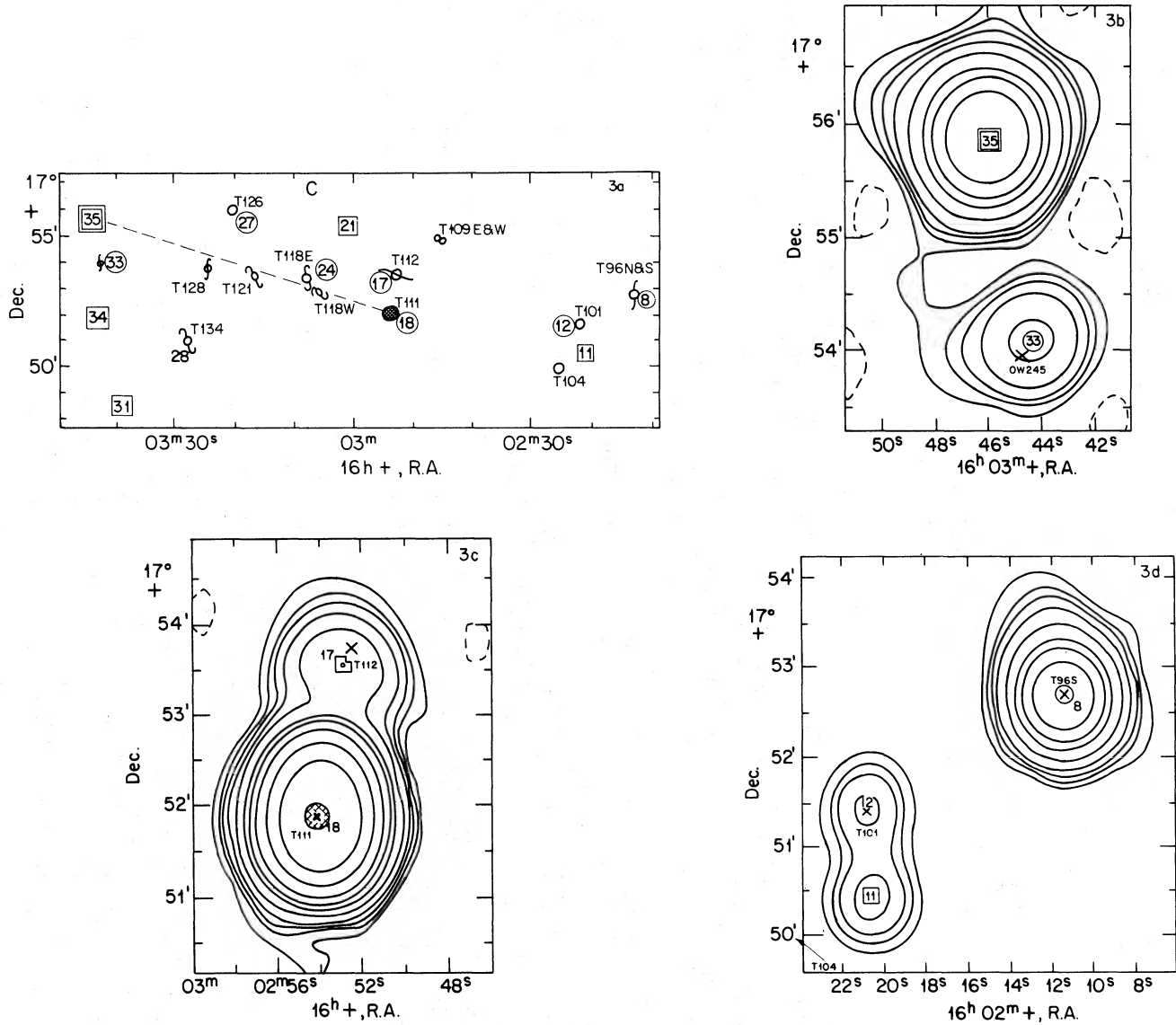


FIG. 3.—Sources near the core of the classic Hercules center. Galaxy numbers preceded by T refer to the list of bright galaxies, circled numbers refer to galaxy-related source numbers in Tables 1 and 2 (hatched circle for $S > 200$ mJy), squares with numbers refer to galaxyless sources in Table 1 (double squares for $S > 50$ mJy). (a) Schematic view for the rectangle C, our choice for the central core. (b)–(d) Contour diagrams for three small regions, with contour levels at +1, +2, 3, 5, 10, 20, 30, 50, 100, and 200 mJy (solid) and at -1 mJy (dashed).

applying a downward correction for missed sources (i.e., after “rounding off the corners” of the square fields) of 25% for $3 \text{ mJy} < S < 9 \text{ mJy}$ and of 10% for $S > 9 \text{ mJy}$, are also given in Table 4.

The strongest discrepancy between observed and expected sources in Table 4 is for the three “galaxyless” sources in the “subcore rectangles” with $S > 50$ mJy (in fact all are above 90 mJy), sources # 35, # 53, and # 63 in C, N, and N, respectively, compared with an expected number of only 0.7 sources (or 1.2 sources for choice S_1). The rectangles also contain more galaxyless sources between 9 mJy and 50 mJy than expected, but the observed/expected ratio is not as large (note that both sources with $20 \text{ mJy} < S < 50 \text{ mJy}$ are in the smallest rectangle, S_3). We also have two negative results in Table 4: (i) There is no excess of observed weak sources ($S < 9 \text{ mJy}$) in the rectangles,

and (ii) in the cluster region outside the rectangles there is no observed excess at any flux level.

While the whole Hercules Supercluster is elongated from S to N, the three subcore rectangles are elongated E to W. Part of this elongation may be due to human prejudice in choosing the rectangle; the fact that the number of sources observed outside the rectangles is actually slightly *smaller* than the expected number of background sources (Table 4) may also be due to some “subconscious cheating” in choosing the rectangles (especially S_3), which unfortunately was done after the observations. However, we have an alternative, more objective criterion for the strongest sources: The position of each of the galaxyless sources (# 35, # 53, and # 63) with $S > 90$ mJy is unequivocal, as are the positions of the very strong radio-emitting galaxies (> 200 mJy), which characterize each of the

clumps (source # 18 in C, # 59 in N, and # 1 in S). The directions of the vectors r from sources 35 to 18, 53 to 59, and 63 to 59 (Figs. 3a and 4a, *thin dashed lines*) indicate the elongation of the clumps; the lengths of the vectors indicate the probabilities of finding a background source as close or closer: Each of the three vectors lies within 20° of the E-W direction, and the "minimum area" $\Sigma\pi r^2$ equals 32% of the total area, 3.5×10^3 arcmin², slightly larger than the combined area of the rectangles C and N. The expected number of background sources over this minimum area is 0.53, compared with three observed.

Entry 66? in Table 1 and in Figure 3c illustrates a phenomenon which has been noted before: Like the sources in Table 4 it is an unresolved source (size $\lesssim 20$ -kpc) not associated with a galaxy; unlike those sources it is in the tail of a head-tail galaxy, and therefore, it is presumably associated with intergalactic gas.

VI. DISCUSSION

Our results, summarized on Table 2, supplement the data available for constructing a joint luminosity function for optical and radio emission from Hercules Cluster galaxies (Jaffe and Perola 1976, Valentijn, Perola, and Jaffe 1977; see also Valentijn 1980, for the Cancer Cluster; Condon and Dressel 1978a, 1978b, and Kotanyi 1980, for the Virgo Cluster). We do not have accurate optical magnitudes for most of our galaxies, but we can make semiquantitative comparisons with

the luminosity function for elliptical galaxies compiled by Auriemma *et al.* (1977). For this comparison we use three sets of galaxies: (1) the 31 "bright" galaxies (from the T-list) with mean apparent magnitude approximately 15.4; (2) the 79 "medium-bright" galaxies from the D-list which are not on the T-list, which we assume have mean apparent magnitude approximately 16.9 (i.e., fainter by a factor of 4); and (3) the 149 "faint" galaxies from the OW-list, which we shall assume have mean magnitude of 18.4 (another factor of 4 fainter). Using a distance modulus of 35.2 for Hercules (to be consistent with Jaffe and Perola 1976), these translate to absolute magnitudes for the three groups of -19.8 (B group), -18.3 (M group), and -16.8 (F group). For these total numbers in the three samples we have counted only once those close pairs and groups of galaxies which would not be resolved on the VLA maps (second entry in first line of Table 3).

Of the first group (B) we have detected three galaxies of types E and S0, and seven of spiral types Sa-Sd, above our flux limit

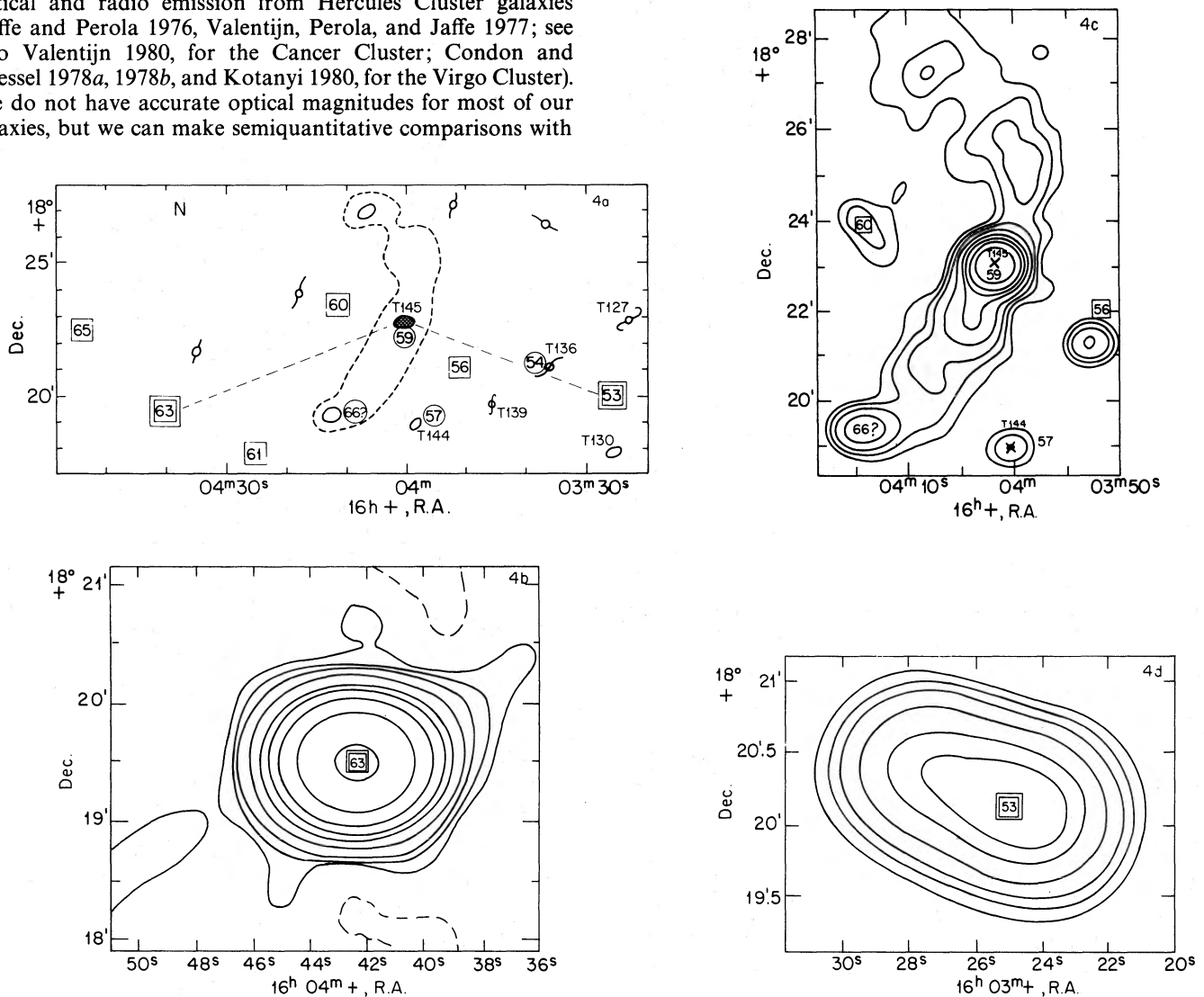


FIG. 4.—Same general notation as for Fig. 3. (a) Schematic view of our choice for the northern subcore, the rectangle N to the north of the classic cluster core. (b)–(d) Contour diagrams for three small regions, with contour levels at +1.5, +3, 5, 10, 20, 30, 50, 100, and 250 mJy (*solid*) and at -1.5 mJy (*dashed*).

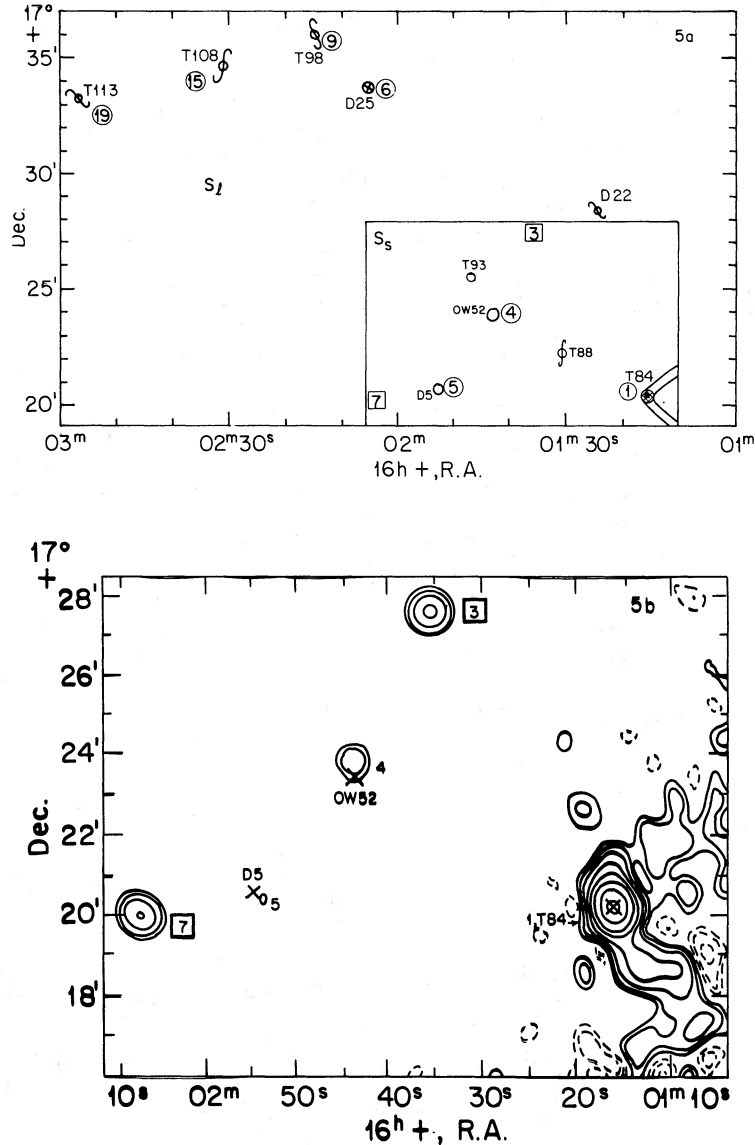


FIG. 5.—Same general notation as for Fig. 3. (a) Schematic view of two alternative choices for the southern subcore: the small rectangle S_s (solid on Fig. 1) containing three bright galaxies, one head-tail source, and two galaxyless sources with flux between 20 and 50 mJy; the large rectangle S_1 (dashed on Fig. 1), containing three additional bright galaxies. (b) Contour diagram for sources in the rectangle S_s , with contour levels at -10 , -5 , -3 mJy (dashed), $+3$, $+5$, 10 , 20 , 40 , 75 , 150 , and 250 mJy (solid). The head-tail source #1 (the galaxy T84) is near a corner of the field, so the data are noisy.

of 1.3 mJy, which translates to $\log P = 21.26$, where P is the galaxy radio power at 1420 MHz in watts Hz^{-1} . Of the second group (M) we have detected five E and S0 galaxies, and eight spirals. Of the third group (F) we detect only one galaxy, whose type has not been determined. We compare these results with Figure 5 of Auriemma *et al.* (1977), which predicts the fraction of galaxies with ratio powers above our threshold to be about 0.22 for $M = -19.8$, 0.038 for $M = -18.3$, and 0.006 for $M = -17.8$. Auriemma *et al.*'s predictions apply to elliptical and S0 galaxies only, of which there are 15 in our B group, 34 in our M group, and 74 in our F group. The numbers predicted and detected are summarized in Table 3. For the E and S0 types, the prediction is significantly in error only for the M group, where we detect more galaxies than expected. It is interesting that the fraction of spirals detected in the B and M groups is somewhat larger than the fraction of ellipticals; in the B group

it is larger by a factor of 2. This suggests that the joint luminosity function for optically bright spirals ($M < -19.5$) is larger than for ellipticals. In the F group we are limited by poor statistics, but we can state that the mean ratio of radio power to optical luminosity for ellipticals in the Hercules Cluster decreases at least as rapidly as in the compilation by Auriemma *et al.* It is also interesting that the fact that we detected only one of the 149 F group galaxies shows that the OW-list is not strongly contaminated by much more distant galaxies. For instance, the bright galaxies in a supercluster 5 times farther away, "hiding behind" A2151, could have mimicked the optical properties of many OW galaxies, but would have led to many more radio detections.

We saw in Figure 2 that the separation θ between the 1.4 GHz and optical image centers is $\lesssim 5''$ for many galaxies. This not only confirms the gratifying result that typical position

TABLE 4
OBSERVED AND EXPECTED NUMBER OF BACKGROUND SOURCES

| SOURCES | S (mJy) | | | |
|----------------------|---------|-----------|-----------|------------|
| | 3-9 | 9-20 | 20-50 | > 50 |
| RECT, observed | 3 | 5 | 2 | 3 |
| RECT, expected | 3.8 | 1.8 (3.4) | 1.1 (2.0) | 0.65 (1.2) |
| OUTS, observed | 15 | 6 | 3 | 0 |
| OUTS, expected | 15 | 7.3 (5.7) | 4.2 (3.3) | 2.5 (1.9) |

NOTE.—Observed number of sources and expected background numbers in various ranges of flux S , for the three combined subclump rectangles (RECT) and the parts of our fields outside the rectangles (OUTS). Sources with galaxies on the OW-list within $40''$ are not included. The expected numbers for the rectangle choice S_1 are given without parentheses, those for S_2 are inside parentheses.

errors on the VLA D configuration are less than $5''$ (§ III) but also gives some information on the nature of the continuum sources. Observations with good resolution in the Virgo Cluster (Kotanyi and Ekers 1983) have shown one extended source displaced from the galaxy center (NGC 4438) by about one-third the galaxy diameter, which corresponds to $\theta \sim 20''$ at the distance of A2151. Our data in Table 2 and Figure 2 show that such phenomena may possibly occur in A2151, but must be rare. Of 16 sources with $S > 3$ mJy only three have θ between $15''$ and $40''$, not much more than expected from unrelated background sources.

Previous authors (Valentijn and Perola 1978; Valentijn 1979a, 1979b) have already discussed the Westerbork data for the two tailed sources (centered on NGC 6034 and NGC 6061) in the light of dynamical models by Jaffe and Perola (1973). Our data give central positions more accurately than the Westerbork data, but our resolution of the tail structure is only slightly better, and we have little to add to the previous authors' discussion of the evidence for intracluster gas and their estimate for the minimum confining pressure. The three strongest galaxyless sources discussed below (#35, #53, and #63) are resolved at the VLA, and the major axis diameters (but not the minor axis ones) should be reasonably reliable. Two of these diameters are slightly smaller than the typical size of features in the tailed sources, and the fluxes of these galaxyless sources are slightly larger than the fluxes in the tail features of NGC 6034 and NGC 6061 (although less than the total flux in these radio galaxies). If similar dynamical models were to be applied to these galaxyless sources as to the tail features, the required minimum confining pressures would presumably be somewhat larger. It is interesting to note that $\theta < 2''$ for both of the tailed sources (#1 and #59), in spite of the fact that the tail's flux centroid is always displaced from the compact head centered on the galaxy's nucleus: the emission on scales of order $1'$ could have come from regions rather far from the head and could already have shown some effects of ram pressure, but there is no evidence for such effects.

Potentially our most interesting result is the statistical data in Table 4 on continuum sources which are more than $40''$ from any galaxy on the extensive OW-list. From the empirical data in Figure 2 the physical association with a galaxy more than $40''$ away seems unlikely. From the correlation of L_r/L_{op} with L_{op} it is very unlikely that the sources in Table 4 are associated with even fainter galaxies than those in the OW-list, unless they involve a physically different phenomenon from ordinary radio galaxies. Thus it is most likely that the five sources with flux $S > 20$ mJy in the three clumps, or subcore rectangles

(RECT), are not directly and primarily associated with individual Hercules galaxies. It is quite possible that they merely represent an upward fluctuation in the number of background sources, since the expected number is two or three, but at least the three strongest of the five sources are extended, which is rare for very distant background sources (Oosterbaan 1978; Katgert 1979). We provisionally adopt the alternative hypothesis that the sources reside in the intergalactic plasma which in turn resides in those portions of the A2151 cluster. This assertion underscores an old puzzle and raises a new one: objects like source 66? in Figure 3c are remarkably compact ($\lesssim 20$ kpc) for a bright galaxy, and the mechanism for the "confinement" is not fully understood. However, 66? resides in the tail of a strong radio galaxy, and the primary energy source is presumably energy production in a large galaxy. Our five galaxyless strong sources are even farther away from bright galaxies, and no "bridges" are visible. It is thus not clear if they have a different source of primary energy, or if even fainter bridges or tails can transport energy over even larger distances (cf. the jets in Cygnus A).

Radio continuum sources seen in random directions, with $S \sim 1$ mJy and no obvious optical galaxy nearby, are usually thought of as extremely bright radio sources at very large redshifts z . If our five sources are typical for other clusters, some of the galaxyless sources with $S \sim 1$ mJy could be situated in cluster cores at intermediate redshifts: Our three strongest galaxyless sources, as well as four galaxy emitters (sources #1, #8, #18, and #59), would have $S \gtrsim 1$ mJy if the Hercules Cluster were moved to $z \sim 0.4$. Angular correlations on the scale of about $1'-10'$ for $S \sim 1$ mJy would then be of interest.

We have claimed the existence of a population of radio sources in clumps inside rich clusters of galaxies, of size $\lesssim 20$ kpc but not associated with bright galaxies. This claim is based on only five sources in A2151 with $S > 20$ mJy (#3, #7, #35, #53, and #63) and is purely provisional, but there may be some corroborating data from the Ursa Major Supercluster (Schuch 1983). For the Virgo Cluster Kotanyi (1980) has shown that there is no very strong effect of this kind (1 Jy in the Virgo Cluster corresponds to only about 15 mJy in A2151), but even here we have some weaker evidence for galaxyless continuum sources in clumps: of 11 Westerbork fields fully mapped at 1.4 GHz (Kotanyi 1980; Kotanyi and Ekers 1983) five (#1, #3, #4, #5, and #11) have two or more sources each with $S > 0.2$ Jy and more than $3'$ from any galaxy brighter than ~ 14 th magnitude. Table 5 gives the number of such sources observed in three flux bins and the expected number of background sources in the five fields, assuming an effective area of 1.2 deg^2 per field. The excess of observed sources is more than would be obtained by choosing the richest five out of 11 random fields for a Poisson distribution of background sources, but it is not clear whether the selection of the 11 fields

TABLE 5
OBSERVED NUMBER OF GALAXYLESS SOURCES IN
FIVE VIRGO CLUSTER FIELDS COMBINED,
IN VARIOUS RANGES OF FLUX, COMPARED WITH
EXPECTED BACKGROUND NUMBERS

| SOURCES | S (Jy) | | |
|----------------|---------|---------|-------|
| | 0.2-0.3 | 0.3-1.0 | > 1.0 |
| Observed | 4 | 6 | 2 |
| Expected | 1.8 | 1.9 | 0.34 |

was fully random or was partly influenced by the presence of strong sources. Even if the sources in Table 5 are in the Virgo Cluster, they represent less total absolute radio luminosity than the five assumed sources in A2151, which in turn emit less than the radio galaxies in A2151. Thus galaxyless cluster sources are not important for the overall energy balance (even if real), but would be interesting physically. A systematic study of a few more nearby clusters would be useful, as would radio observations at higher angular resolution of the five sources in A2151 and more detailed optical searches.

It is also useful to compare our results with the recent *IRAS* survey of the Hercules Cluster (Young *et al.* 1984). The resolution of the *IRAS* study is fine enough to identify the infrared sources with D-list galaxies in most cases, although there is sometimes confusion, e.g., for Young *et al.*'s source number 17b, which we shall assume corresponds in fact to D155. Comparing our Table 2 with their Table 1, we have the following statistics for spiral galaxies: Of the 16 B galaxies they detected 8 at 60 μ m, and we detected 7 at 21 cm with 6 detections in common; of the 45 M galaxies they detected 11, and we detected 8 with 6 detections in common. The probability of drawing that many elements (or more) in common from two unrelated random samples is only ~ 0.01 for the bright galaxies and 1.3×10^{-3} for the medium-bright galaxies. The strong correlation between the 60 μ m flux and the 21 cm flux (the mean flux ratio is ~ 80) is shown in Figure 6.

Radio continuum emission for nearby spirals is correlated with $H\alpha$ emission, a measure of the prevalence of H II regions (Kennicutt 1983). Most of the radio emission is probably synchrotron radiation from supernova remnants (rather than thermal bremsstrahlung), but supernova and H II region occurrence rates should both be proportional to the current formation rate of massive stars. Our radio correlation with the far-infrared flux for Hercules spirals is gratifying, since the far-IR flux is expected to be correlated with the current luminosity of O and B stars (our correlation seems to be even tighter than Kennicutt's possibly because the far-IR suffers less from obscuration than the $H\alpha$). Few E and S0 galaxies were detected at 60 μ m, with only one detection in common (T126). This

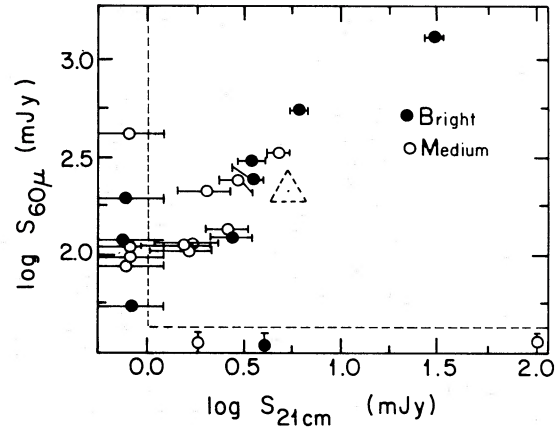


FIG. 6.—The relationship between radio (21 cm) and infrared (60 μ m) flux for Hercules Cluster spiral galaxies. Optically bright spirals (B sample) are represented by different symbols from fainter galaxies (M group). Upper limits are shown by the points along the left and bottom axes. The correlation suggests a ratio of 60 μ m to 21 cm fluxes of about 80 to 1. The dashed triangle refers to D78 (T126), the only joint detection for E or S0 galaxies.

absence of correlation is also expected, since radio emission from ellipticals is thought to be caused by accretion in galactic nuclei (Condon and Dressel 1978a) which is not related to present-day star formation.

We are particularly indebted to Drs. Okamura and Wakamatsu for providing us with their list of galaxies, which was extremely helpful in the analysis of our data. We are also grateful to Drs. G. Bothun, J. Condon, L. L. Dressel, A. Dressler, R. D. Ekers, R. Kennicutt, C. Kotanyi, W. J. Jaffe, T. Jones, L. Rudnick, and E. Valentijn for interesting discussions and suggestions and to Cindy Miller for help with the data analysis. This work was supported in part by NSF grants AST 81-16370 to Cornell University and AST 82-16879 to the University of Minnesota and by a grant from the Graduate School, University of Minnesota.

REFERENCES

- Auriemma, C., Perola, G., Ekers, R., Fanti, R., Lari, C., Jaffe, W., and Ulrich, M. 1977, *Astr. Ap.*, **57**, 41.
 Bothun, G. D. 1981, Ph.D. thesis, University of Washington.
 Condon, J. J., and Dressel, L. L. 1978a, *Ap. J.*, **221**, 456.
 ———. 1978b, *Ap. J.*, **222**, 745.
 Condon, J. J., and Mitchell, K. J. 1982, *A. J.*, **87**, 1429.
 Dressler, A. 1980, *Ap. J. Suppl.*, **42**, 565.
 Jaffe, W. J., and Perola, G. C. 1973, *Astr. Ap.*, **26**, 423.
 ———. 1975, *Astr. Ap. Suppl.*, **21**, 137 (JP).
 ———. 1976, *Astr. Ap.*, **46**, 275.
 Katgert, J. K. 1979, *Astr. Ap.*, **73**, 107.
 Kennicutt, R. 1983, *Astr. Ap.*, **120**, 219.
 Kotanyi, C. G. 1980, *Astr. Ap. Suppl.*, **41**, 421.
 Kotanyi, C. G., and Ekers, R. D. 1983, *Astr. Ap.*, **122**, 267.
 Okamura, S., and Wakamatsu, K. 1983, preprint.
 Oosterbaan, C. E. 1978, *Astr. Ap.*, **69**, 235.
 Perola, G. C., and Valentijn, E. A. 1979, *Astr. Ap.*, **73**, 54.
 Schuch, N. J. 1983, *M.N.R.A.S.*, **204**, 1245.
 Tarengi, M., Tift, W., Chincarini, G., Rood, H., and Thompson, L. 1979, *Ap. J.*, **234**, 793.
 ———. 1980, *Ap. J.*, **235**, 724.
 Thompson, A. R., Clark, B. G., Wade, C. M., and Napier, P. J. 1980, *Ap. J. Suppl.*, **44**, 151.
 Valentijn, E. A. 1979a, *Astr. Ap.*, **78**, 362.
 ———. 1979b, *Astr. Ap.*, **78**, 367.
 ———. 1980, *Astr. Ap.*, **89**, 234.
 Valentijn, E. A., and Perola, G. 1978, *Astr. Ap.*, **63**, 29.
 Valentijn, E. A., Perola, G., and Jaffe, W. 1977, *Astr. Ap. Suppl.*, **28**, 333.
 Young, E., *et al.* 1984, *Ap. J. (Letters)*, **278**, L75.

JOHN M. DICKEY: Department of Astronomy, University of Minnesota, Minneapolis, MN 55455

EDWIN E. SALPETER: Center for Radiophysics and Space Research, 424 Space Science Bldg., Cornell University, Ithaca, NY 14853